AD-A077 280 NATIONAL AEROSPACE LAB AMSTERDAM (NETHERLANDS) F/G 20/9
A FAST PARABOLIC MODULE FOR THE SOLUTION OF MHD CHANNEL FLOW EQ--ETC(U)
FEB 77 J P LINDHOUT , H SNEL , W F MERCK

UNCLASSIFIED NLR-MP-77006-U NL

| OF |
ADA
077280

END
DATE
FILMED
12-79
DDC

NATIONAAL LUCHT- EN RUIMTEVAARTLABORATORIUM

NATIONAL AEROSPACE LABORATORY NLR

THE NETHERLANDS

NLR MP 77006 U

A FAST PARABOLIC MODULE FOR THE SOLUTION OF MHD CHANNEL FLOW EQUATIONS BETWEEN ELECTRODE WALLS

BY

J.P.F. LINDHOUT, H. SNEL AND W.F.H. MERCK

DOCUMENT CONTROL SHEET

	ORIGINATOR'S REF.		SECURITY CLASS.
(14)	NLR-MP-77006-U		Unclassified

ORIGINATOR National Aerospace Laboratory NLR
Eindhoven University of Technology

(6)

TITLE A fast parabolic module for the solution of MHD channel flow equations between electrode walls.

(11) 25 Feb 77 (12) 24

PRESENTED AT
International Symposium on Innovative Numerical Analysis in Applied Engineering Science, Versailles, France, May 23-27, 1977

(10) AUTHORS	DATE	pp	ref
J.P.F. Lindhout, H. Snel (NLR) W.F.H. Merck (EUT)	25-II-1977	21	17

DESCRIPTORS

Energy conversion	Numerical Analysis
Magnetohydrodynamic flow	Boundary Layer Equations
Ducted flow	Boundary value problems
Spline functions	Interpolation
Parabolic differential equations	Non-linear equations
Approximation	Stability

ABSTRACT

Two forth-order methods, based on cubic-splines approximations, are proposed to solve parabolic differential equations. The cubic-splines approximation has a second-order accuracy, which is improved in both methods to fourth-order in different ways. In the first method, the second-order truncation term is estimated by differentiating twice the basic equations. In the other method a local Richardson extrapolation is applied at each marching station to obtain fourth-order accurate values at every two points; subsequent quintic Hermite interpolation is then used to obtain equally accurate values at the remaining points. A von Neumann stability analysis shows that the methods are unconditionally stable. Both methods are applied to a simple boundary-layer problem. The method with local Richardson extrapolation is employed to solve simultaneously the continuity and energy equation describing the behaviour of the electron gas along the cathode wall in an MHD channel. The results indicate that it is worthwhile to reconsider the model of the electrode-plasma interface.

NLR MP 77006 U

A FAST PARABOLIC MODULE FOR THE SOLUTION OF MHD CHANNEL FLOW EQUATIONS BETWEEN ELECTRODE WALLS

by

J.P.F. Lindhout, H. Snel
National Aerospace Laboratory N.L.R., Amsterdam, The Netherlands

W.F.H. Merck
Eindhoven University of Technology, Eindhoven, The Netherlands

Paper presented at the International Symposium on Innovative Numerical Analysis in Applied Engineering Science, Versailles, France, May 23-27 1977.

21 pages

Division: Sc. Serv.
Prepared: JPFL
Approved: WL/

Completed: 25 February 1977
Ordernr. : 554.401
Typ. : hvlk

A FAST PARABOLIC MODULE FOR THE SOLUTION OF MHD CHANNEL FLOW EQUATIONS BETWEEN ELECTRODE WALLS

by J.P.F. Lindhout
H. Snel
W.F.H. Merck

1. INTRODUCTION

The present study is part of the NLR research program aimed at generating numerical solutions of Magnetic Hydrodynamic (MHD) duct flow. This research program is incorporated in the investigations into plasma-flow phenomena, which are performed in the Group Direct Energy Conversion of the EUT.

MHD energy conversion is a process in which the motion and the thermal energy of an electrically conducting fluid through an applied magnetic field perpendicular to the motion is converted into electrical energy. This process yields higher conversion efficiences than conventional processes. A schematic view of an MHD generator channel is given in fig. 1. The channel is horizontally bounded by insulator walls and in the vertical direction by electrode walls in which segmented electrodes are placed.

The magnetic field B is applied perpendicular to the insulator walls. The induced electrical field E equals the vector product uxB. It produces a current in the conducting medium which flows through the electrodes.

The complete system of equations describing the phenomena can be divided into three groups:

i) the gasdynamical - or global equations
ii) the electron-gas equations
iii) the electromagnetic field equations.

The first two groups of equations are of parabolic type. Parabolic equations in fluid dynamics frequently characterize situations in which the dependent variables have large gradients normal to the main flow direction.

For this type of equations, two fourth-order accurate solution methods are presented. Both methods are based on cubic-spline representation of the dependent variables normal to the marching direction. A stability analysis will be given and, to show the accuracy, both methods are applied to a simple flow problem, of which the exact solution is known.

One of the fourth-order-spline methods is used to solve the electron-gas equations which have substantially more complex boundary conditions than the global-gas equations. Spline methods are preferable in situations like this where derivatives enter the boundary conditions.

A second-order difference scheme was already applied by the present authors to solve the global-gas equations between insulator walls (ref. 1).

2. CUBIC-SPLINE SOLUTION OF PARABOLIC DIFFERENTIAL EQUATIONS

Rubin and Graves (ref. 2) introduced the application of collocational cubic splines to the solution of parabolic partial differential equations. For two-dimensional problems, conventional finite differencing took place in the marching direction. The resulting two-point-boundary-value problem, normal to the marching direction, was solved by cubic splines. The spline is required to satisfy the second-order differential equation at each grid point. Applying the spline continuity relations one can obtain a block tridiagonal system of equations for the function values, say u, its first (m) and second derivatives (M) in the normal direction. This method is of second-order accuracy in u and m, because errors in M itself are, according to the cubic-spline approximation, proportional to the square of the interval width.

Daniel and Swartz (ref. 3) suggested a method of obtaining fourth-order accuracy for two-point-boundary-value problems, basically by eliminating the second-order truncation error in M, which is $h^2(\partial^4 u/\partial y^4)/12+0(h^4)$. For the inner points, the leading term of the truncation error was approximated by means of second-order central differences of M. At the boundary points non central differences had to be used. The collocation equations contained information of other points and the resulting equations could only be reduced to a five-diagonal system.
Rubin and Khosla (ref. 4) explored this method extensively for parabolic equations.

To demonstrate the details of both proposed methods, the boundary layer equations of an incompressible fluid near a stagnation point are solved. The governing flow equations can be written as follows:

conservation of momentum: $u(\partial u/\partial x)+v(\partial u/\partial y)=u_e(du_e/dx)+\nu(\partial^2 u/\partial y^2)$, (1)

conservation of mass : $(\partial u/\partial x)+(\partial v/\partial y) =0$, (2)

in which x and y form a Cartesian coordinate system, u and v are velocities in x- and y-direction, ν is the known viscosity, u_e is the given velocity at the edge of the boundary layer. When equation (1) is used, equation (2) can be replaced by:

$$\partial (v/u)/\partial y= - \left\{u_e(du_e/dx)+\nu(\partial^2 u/\partial y^2)\right\}/u^2, \tag{3}$$

in which only y-derivatives of the unknowns occur. The boundary conditions are:

$y = 0$: $u = 0$, $v = 0$ (4a)

$y = \infty$: $u = u_e$ (4b)

When stagnation conditions are assumed, i.e. (du_e/dx) is constant, a similarity solution of (1) and (2) exists, which permits the determination of the accuracy of the proposed methods (ref. 5). A grid is assumed at which a grid function u_i^j exists: $u_i^j=u(x=i.k,\ y=(j-1).h)$. Equation (1) is centered at the grid point (i+1, j). The derivative in the marching direction is approximated by the second-order difference formula:

$$\partial u/\partial x \sim (3u_{i+1}^j - 4u_i^j + u_{i-1}^j)/(2k), \tag{5}$$

which is substituted in (1). The non-linear terms at the level i+1, in the resulting equation are linearised: $(u_{i+1}^j)^2$ by the Newton-Raphson method and for v_{i+1}^j in $v_{i+1}^j(\partial u/\partial y)_{i+1}^j$ the value of the last iteration is taken.

Equation (1) can be written with the help of equation (5) and the linearizing techniques, as an ordinary differential equation:

$$a_j\, h^2(\partial^2 u/\partial y^2)_{i+1}^j + b_j h(\partial u/\partial y)_{i+1}^j + c_j\, u_{i+1}^j = d_j, \tag{6}$$

$(i=1,2,\ldots,\ j=1(1)N,\ N \text{ odd})$

in which a, b, c, d are functions of h, u_e (du_e/dx) and the last iterate of the unknowns u and v.

At each collocation point the following approximations are made:

$$(\partial u/\partial y)^j_{i+1} \sim m^j_{i+1}, \quad (\partial^2 u/\partial y^2)^j_{i+1} \sim M^j_{i+1}, \tag{7a,b}$$

where m and M are the first and second derivative, resp. of the cubic spline. According to Ahlberg, Nilson and Walsh (ref. 6), the first approximation is fourth-order accurate and the last one second-order accurate.

From the equidistant cubic-spline approximation of u, it is possible to deduce the following four indepent equations for u, m and M at three adjacent grid points (ref. 6):

$$M^{j-1} = 6(u^j - u^{j-1})/h^2 - 2(m^j + 2m^{j-1})/h, \tag{8a}$$

$$M^j = 3(u^{j+1} - 2u^j + u^{j-1})/h^2 - (m^{j+1} - m^{j-1})/h, \tag{8b}$$

$$M^{j+1} = -6(u^{j+1} - u^j)/h^2 + 2(2m^{j+1} + m^j)/h \tag{8c}$$

$$u^{j+1} - u^{j-1} = h(m^{j+1} + 4m^j + m^{j-1})/3; \tag{8d}$$

for convenience the subscript i+1 is omitted.

These equations are employed to approximate m and M. To demonstrate this we write equation (6) for j-1, j and j+1 together with equation (8) as a vector equation:

$$A_j U^{j-1} + B_j U^j + C_j U^{j+1} = D_j, \quad j = 2\ (1)\ N-1 \tag{9}$$

in which: $U^j = (h^2 M^j, hm^j, u^j)^T$

$$D_j = (d_{j-1}, d_j, d_{j+1}, 0, 0, 0, 0)^T,$$

and

$$A_j = \begin{pmatrix} a_{j-1} & b_{j-1} & c_{j-1} \\ 0 & 0 & 0 \\ 0 & 0 & 0 \\ -1 & -4 & -6 \\ 0 & 1 & 3 \\ 0 & 0 & 0 \\ 0 & 1 & 3 \end{pmatrix} \quad B_j = \begin{pmatrix} 0 & 0 & 0 \\ a_j & b_j & c_j \\ 0 & 0 & 0 \\ 0 & -2 & 6 \\ -1 & 0 & -6 \\ 0 & 2 & 6 \\ 0 & 4 & 0 \end{pmatrix} \quad C_j = \begin{pmatrix} 0 & 0 & 0 \\ 0 & 0 & 0 \\ a_{j+1} & b_{j+1} & c_{j+1} \\ 0 & 0 & 0 \\ 0 & -1 & 3 \\ -1 & 4 & -6 \\ 0 & 1 & -3 \end{pmatrix}$$

By premultiplication of (9) by a suitable row vector $r = (r_1,..r_7)$ it is possible to obtain a scalar equation with only three unknowns. In order to extract from (9) an equation in which only the function values u^{j-1}, u^j and u^{j+1} occur and no derivatives, r has to satisfy:

$$rA_j^1 = rA_j^2 = rB_j^1 = rB_j^2 = rC_j^1 = rC_j^2 = 0 \qquad (10)$$

in which the superscript the involved column indicates.
Now r is fully determined by (10), except for a multiplicative constant, and after multiplication of (9) by the chosen r we obtain:

$$\alpha_j u^{j-1} + \beta_j u^j + \gamma_j u^{j+1} = \rho_j \qquad j = 2(1)N \qquad (11a)$$

Mixed boundary conditions of the type:

$$a_o h^2 M_1 + b_o h m_1 + c_o u_1 = d_o \qquad (12)$$

can be handled by the same technique. System (9) is extended with the boundary condition by extending the matrices A, B, C and vector D by appropriate elements. By premultiplication of a new row vector r, now with eight elements, one can obtain:

$$\beta_1 u^1 + \gamma_1 u^2 = \rho_1 \qquad (11b)$$

r has to satisfy (10) and moreover:

$$rC_j^3 = 0.$$

Mixed boundary conditions at the upper boundary can be treated equivalently and lead to:

$$\alpha_N u^{N-1} + \beta_N U^N = \rho_N \qquad (11c)$$

The tri-diagonal system (11) can be solved with standard algorithm's for u^j. The m^j can be solved from equation (6) and (8c). An initial condition for m at the lower boundary is obtained in the same fashion as (11b). M in its turn follows from the original differental equation. All quantities are derived second order accurate in h.

To obtain fourth-order accurate results equation (6) is solved once again with stepsize 2h in the y-direction, while only the odd points of the grid are used.
The first solution is indicated by $*$ and by $\sim$ the solution in which only the odd points are used. The leading term of the truncation error of the results of odd points is four times as large as the results of the first

solution for all points. Richardson-extrapolation consists in finding a more accurate result at the odd points by elimination of the leading truncation term:

$$\varphi = (4\varphi^* - \tilde{\varphi})/3, \tag{13}$$

in which φ stands for u^j_{i+1}, $(\partial u/\partial y)^j_{i+1}$, and $(\partial^2 u/\partial y^2)^j_{i+1}$, j=1(2)N.
In the further computations, it is necessary to obtain results at the even points as accurate as those at the odd points along a normal. This is accomplished in the following way:
The function values and the first and second derivatives at the odd points hold exactly enough information to define a quintic hermite polynomial over the intervals between each pair of successive odd points.

At the even points, the quintic polynomial is used to interpolate the unknowns:

$$u^j=(u^{j-1}+u^{j+1})/2+5h\left\{(\partial u/\partial y)^{j-1}-(\partial u/\partial y)^{j+1}\right\}/16+h^2\left\{(\partial^2 u/\partial y^2)^{j+1}+(\partial^2 u/\partial y^2)^{j-1}\right\}/16, \quad j=2(2)N-1, \tag{14}$$

$$(\partial u/\partial y)^j=-15(u^{j-1}-u^{j+1})/16h-7\left\{(\partial u/\partial y)^{j-1}+(\partial u/\partial y)^{j+1}\right\}/16+ -h\left\{(\partial^2 u/\partial y^2)^{j-1}-(\partial^2 u/\partial y^2)^{j+1}\right\}/16, \quad j=2(2)N-1, \tag{15}$$

$$(\partial^2 u/\partial y^2)^j=-3\left\{(\partial u/\partial y)^{j-1}-(\partial u/\partial y)^{j+1}\right\}/4h-\left\{(\partial^2 u/\partial y^2)^{j-1}+ + (\partial^2 u/\partial y^2)^{j+1}\right\}/4, \quad j=2(2)N-1. \tag{16}$$

The idea of applying Richardson-extrapolation to improve the results of numerical techniques is not new. Richardson-extrapolation is employed for several years, e.g., in the box method of Keller (ref. 7), for the computation of 2D and 3D boundary layer flows.

The new feature here is that, in the case of the cubic-spline solution, it is permitted to apply Richardson-extrapolation for each marching step before the computation is proceeded to the next x-station.

The second method presented here eliminates the truncation term $h^2(\partial^4 u/\partial y^4)/12$ of equation (7b). By differentiating the original equation (1) twice, we can express $\partial^4 u/\partial y^4$ in second and lower derivatives, and we can approximate the second derivative in (1) at each collocation point by:

$$\partial^2 u/\partial^2 y \sim M - h^2\{(uv/\nu+m)(\partial m/\partial x)+(v^2/\nu-\partial u/\partial x)M+u(\partial M/\partial x)\}/12\nu+O(h^4) \qquad (17)$$

The x-derivatives in (17) are approximated in the same way as described already for $\partial u/\partial x$. The non-linear terms are linearized in the Newton-Raphson fashion, except for the terms in which v appears, which are taken from the most recent iteration. The resulting linear equation in u, m, and M can further be treated in exactly the same way as in the cubic-spline case. It is necessary to store also m and M at three successive x-stations. Unlike the method of ref. (3) the use of unsymmetrical differences at the wall is avoided; this can be an important advantage in the case of steep gradients. The fact that a tri-diagonal system of equations results from this method is also a clear advantage. However, the differentiation can be a tedious task. For complicated equations the use of computerised formula manipulation can be of great help.

At this point, it is clear that either of the two methods have yielded values for u and its derivatives. The RHS of equation (3) can be computed and equation (3) can be written as a first-order differential equation in the unknown (v/u). The solution procedure can be the same as that used for the cubic-spline solution of (6) if an additional boundary condition is given. It is consistent with the asymptotic behaviour of (1) and (2) to apply:

$$y = (N-1).h \quad : \quad \partial^2(v/u)/\partial y^2 = 0 \qquad (18)$$

Because in (3) the second derivative is missing, the solution of (3) is fourth-order accurate.

For several stepsizes h in y-direction, computations are performed starting at x=0.1 untill x=1.0, k=0.01. The error exhibited at the last x-station in the friction coefficient c_f is depicted in fig. 2 for the two methods presented. For comparison results obtained by aplication of the cubic-spline method and a simple difference scheme are included. From the slope of the curves, it can be inferred that the cubic-spline method and the difference method are second-order accurate indeed. Both methods proposed are fourth-order accurate, except for the first one in the case of a very small number of netpoints.

3. STABILITY ANALYSIS

We examine the stability properties of the presented fourth-order methods using the simple parabolic equation:

$$u_x = \sigma u_{yy} \qquad (19).$$

s does not imply a severe restriction of the analysis, because the highest ivatives are retained.

u_x is discretized according to (6), the following equation at each collo-ion point is obtained:

$$3u^j_{i+1}-2k\sigma(\partial^2u/\partial y^2)^j_{i+1}=4u^j_i-u^j_{i-1}. \qquad (20)$$

s equation can be solved by:

i) the cubic-spline method, for short: CS-method

ii) the method in which two cubic-spline solutions are used to reduce the truncation error by Richardson-extrapolation, followed by quintic hermite interpolation for the even points, for short: RH-method

iii) the method in which the truncation error is reduced by estimation of the truncation error by differentiation, for short: D-method.

CS-method: Application of equations (7b)-(8c)permits the elimination of m's and M's, which gives rise to the following equation in u:

$$3(u^{j-1}_{i+1}+4u^j_{i+1}+u^{j+1}_{i+1})-12(k/h^2)\sigma(u^{j-1}_{i+1}-2u^j_{i+1}+u^{j+1}_{i+1}) =$$

$$4(u^{j-1}_i+4u^j_i+u^{j+1}_i)-(u^{j-1}_{i-1}+4u^j_{i-1}+u^{j+1}_{i-1}). \qquad (21)$$

The stability of this scheme can be investigated by the von Neumann method. Because (21) is a three-level scheme, the analysis leads to a second-order amplification matrix (ref. 8). The Fourier-decomposition of u can be written as:

$$u^j_i = \xi 1_i \exp(\hat{\imath}jnh) \qquad (22)$$

in which $\hat{\imath}$ is the imaginary unit and n the wave number. Substitution of (22) into (21) gives a scalar equation in $\xi 1_{i+1}$, $\xi 1_i$ and $\xi 1_{i-1}$ which can be transformed into a vector equation by the introduction of $\xi 2$:

$$\xi 2_{i+1} = \xi 1_i \qquad (23)$$

The resulting vector equation is given by:

$$\xi_{i+1} = A\,\xi_i \ , \qquad (24)$$

amplification matrix $A = \begin{pmatrix} 4/r & -1/r \\ 1 & 0 \end{pmatrix}$ and $\xi = (\xi_1, \xi_2)^T$,

The eigenvalues of A satisfy the following quadratic equation:

$$r\lambda^2 - 4\lambda + 1 = 0 \tag{25}$$

If $3 \leqslant r < 4$, the roots of (25) are positive and smaller than or equal to one. If $r \geqslant 4$, the roots are the complex conjugate of each other, and it follows at once that:

$$|\lambda_1|^2 = |\lambda_2|^2 = \lambda_1 \bar{\lambda}_1 = \lambda_1 \lambda_2 = {}^1/r \leqslant {}^1/4 \tag{26}$$

Consequently it can be concluded that the CS-method is unconditionally stable.

ii) The RH-method: The results of the CS-method at all points, with step-size h, are indicated by $*$ and the solution at odd points, stepsize 2h is indicated by $\sim$. The amplification matrix for the fourth-order accurate results at the odd points is constructed according to equation (13):

$$A_{odd} = \begin{pmatrix} \frac{4}{3}({}^4/r^* - {}^1/\tilde{r}) & -{}^1/3({}^4/r^* - {}^1/\tilde{r}) \\ 1 & 0 \end{pmatrix} \tag{27}$$

Its eigenvalues satisfy also the quadratic equation (25); the leading term can then be expressed as:

$$r_{odd} = 3 + \frac{12\left[(k/h^2)\sigma(1-\cos\psi)/(2+\cos\psi)\right]^2}{1+5(k/h^2)\sigma(1-\cos\psi)/(2+\cos\psi)} \tag{28}$$

With the same reasoning as above we can proof that the moduli of the eigenvalues are equal to or less than one.

To examine the stability of the even points, a Fourier decomposition of m and M of the cubic-spline solution is assumed:

$$\begin{aligned} m_i^j &= \eta 1_i \exp(\hat{\imath} j\psi)/h, \\ M_i^j &= \mathfrak{H}1_i \exp(\hat{\imath} j\psi)/h^2 \end{aligned} \tag{29}$$

From equations (8), the following relations can be derived between the Fourier-coefficients of m and M and those of u:

$$\begin{aligned} \eta 1 &= 3\hat{\imath}\sin\psi/(2+\cos\psi)\,\xi_1, \\ \mathfrak{H}1 &= -6(1-\cos\psi)/(2+\cos\psi)\,\xi_1 \end{aligned} \tag{30}$$

It can be shown that these relations also hold for the fourth-order accurate results at the odd points. Substitution of the three Fourier-decompositions and equation (30) into equation (14) gives the connection between the eigenvalues of the odd and the even amplification matrix:

$$|\lambda_{even}| = \left\{5-(5-\cos\psi)^2 / 8\right\}/(2+\cos\psi)\ |\lambda_{odd}| \qquad (31)$$

Hence the moduli of the even eigenvalues are equal to or less than the odd ones.

In fig. 3, the eigenvalues are depicted for the three cases treated in this chapter. The conclusion can be drawn that the RH-method is unconditionally stable.

iii) D-method: The introduction of a better approximation for $\partial^2 u/\partial y^2$ with respect to the CS-method does not change the stability analysis because only higher-order terms are added, which have no influence upon the stability.

4. THE ELECTRON GAS EQUATIONS

The RH-method is used to solve the electron gas equations along the electrode wall of an MHD channel. This exercise seems to be of sufficient difficulty to test the method in practical circumstances.

The electron gas equations are derived from the physical model of and MHD-duct, as used for electric power generation, with argon as a working medium seeded with a small fraction of cesium vapour to increase the electrical conductivity. The current-carrying electrons are created by ionization of the Cs, consequently the plasma consists of electrons, CS-ions, Cs-atoms and Ar-atoms. Because there is little interaction between the electrons and the abundant Ar-atoms, the electrons behave as a separate gas, with specific electron gas temperature T_e (ref. 9, 10, 11, 12).

The interaction of the Ar-Cs plasma with the applied magnetic field introduces a Lorentz force in the global momentum equation, and enthalpy extraction and ohmic dissipation terms in the global energy equation. These equations are not dealt with in this paper; the gasdynamic quantities p, u, v, T are supposed to be known.

Here the solution of the electron gas equations is emphasised, because they offer the heaviest problems in numerical computations. These problems are generated by the steep gradients at the wall and by the exponential relations between the coefficients of the differential equations and the electron

Morecver the electron gas tends to be unstable, which is caused by a positive feedback process called ionization instability. This can be dealt with by the use of effective, time-averaged, values for electrical conductivity (σ_{eff}) and Hall parameter (β_{eff}) (ref. 11).

In our model, turbulent terms are omitted and the electrode wall is infinitely segmented, which results in an axial current component $J_x=0$. Non-equilibrium ionization and ambipolar diffusion are taken into account in the electron gas equations, which are merely stated here (ref. 13, 14):

continuity

$$u(\partial C_e/\partial x) + v(\partial C_e/\partial y) = m_e \overset{\circ}{n}_e + (\mu/S)(\partial^2/\partial y^2)\left\{C_e(1+T_e/T)\right\} \quad (32)$$

energy

$$\begin{aligned}\rho\, c_{v,e}\, C_e\left\{u(\partial T_e/\partial x)+v(\partial T_e/\partial y)\right\} &= \tfrac{2}{3}c_{v,e}C_eT_e\left\{u(\partial\rho/\partial x)+v(\partial\rho/\partial y)\right\} + \\ J_y^2/\sigma_{eff} - H_b(T_e-T)+(\partial/\partial y)\Big[\,3(k/e)^2T_e\sigma_{eff}(\partial T_e/\partial y)+2.5kT_e\mu/(m_eS)\cdot & \\ \partial\left\{C_e(1+T_e/T)\right\}/\partial y\Big] - 1.5kT_e(\partial/\partial y)\Big[\mu/(m_eS)\partial\left\{C_e(1+T_e/T)\right\}/\partial y\Big] + & \\ - \overset{\circ}{n}_e(E_I+c_{v,e}m_eT_e) &\end{aligned} \quad (33)$$

The symbols used in these equations are:

$C_e = n_e m_e/\rho$, electron gas-concentration

n_e = number density of electrons

$\overset{\circ}{n}_e = n_e(n_s-n_e)6.22_{10}^{-18}\, T_e^{3/2}\, \exp(-2.556\, e/kT_e) +$

$\quad -n_e^3 2.58_{10}^{-39}\exp(1.337e/kT_e)$, electric source term

m_e = mass of an electron

n_s = number density of seed particles

n_a = number density of argon

μ = viscosity

E_I = ionization energy of Cs

e = charge of an electron

k = constant of Boltzmann

J_y^2/σ_{eff} = ohmic dissipation

J = current density

$\sigma_{eff} = \sigma$ if $\beta \leq \beta_{crit}$, otherwise $\sigma_{eff} = \sigma/\beta_{crit}/\beta$; $\beta = eB/m_e\nu_c$,

$\beta_{crit}=1.5$, $\sigma = \dfrac{e^2 n_e}{m_e \nu_c}$

$\frac{1}{m_e} \frac{\mu}{S} \frac{\partial}{\partial y}\left\{C_e(1+T_e/T)\right\}$ = ambi-polar ion flux

$H_b = 3\rho C_e k\left[\frac{\nu_{e,i}+\nu_{e,as}}{m_s} + \frac{\nu_{e,aa}}{m_a}\right]$, collision term

m_a = mass of an argon atom

m_s = mass of a seed particle

S = Schmidt number

$\nu_c = \nu_{e,i} + \nu_{e,as} + \nu_{e,aa}$

$\nu_{e,i} = 1.55_{10}^{-6} n_e T_e^{-\frac{3}{2}} \ln\left\{8.76_{10}^{6}(T_e^3/n_e)^{\frac{1}{2}}\right\}$, collision frequency electron-Cs-ion

$\nu_{e,aa} = \frac{1}{2}10^{-20} n_a(8kT_e/\pi m_e)^{\frac{1}{2}}$, collision frequency electron-Ar-atom

$\nu_{e,as} = \frac{1}{2}10^{-17} (n_s-n_e)(8kT_e/\pi m_e)^{\frac{1}{2}}$, collision frequency electron-Cs-atom

The energy transport term perpendicular to the wall contains electron heat conduction, heat transport by electric current and ambi-polar diffusion.

The boundary conditions are at the center line of the duct:

$$\partial C_e/\partial y = \partial T_e/\partial y = 0 \tag{34}$$

At the wall, a two-layer model is used. It is assumed that adjacent to the wall a collision-less electrostatic sheath exists which is directly bounded by the continuum plasma (ref. 13, 14, 15, 16). This model leads to the wall boundary conditions:

$$(T+T_e)(\partial C_e/\partial y)+\left\{(\partial T_e/\partial y) - \frac{T_e}{T}(\partial T/\partial y) - \frac{\rho S}{\mu}\left(\frac{kT}{2\pi m_s}\right)^{\frac{1}{2}} T\right\} C_e = 0 \tag{35}$$

and:

$$\left[J_y/e+(\rho C_e/m_e)\left(\frac{kT}{2\pi m_s}\right)^{\frac{1}{2}}\right]\left[\frac{1}{2} - \frac{e\Delta\varphi}{kT_e}\right] + \frac{3k}{e^2}\sigma_{eff}\frac{\partial T_e}{\partial y} = 0 \tag{36}$$

for y=0, where the sheath voltage drop

$$\Delta\varphi = -\frac{kT_e}{e}\ln\left[\frac{J_y-J_{em}}{n_e e}\left(\frac{2\pi m_e}{kT_e}\right)^{\frac{1}{2}} + \left(\frac{Tm_e}{T_e m_i}\right)^{\frac{1}{2}}\right] \tag{37}$$

In order to solve (32) and (33) with the appropriate boundary conditions, the x-derivatives are approximated according to equation (5).

Equations (32) and (35) are linearized with respect to C_e and its derivatives in Newton-Raphson fashion. For T_e and its derivatives the last iterates are taken. This results in a linear two-point-boundary-value problem in C_e, which is solved by the RH-method. Subsequently, the same quasi Newton-Raphson process is applied to equation (33) and (36) to solve T_e and its derivatives. To deal with the steep gradients near the wall, a suitable transformation was introduced to stretch the wall region:

$$\eta = (a+y/y_{max})^{1/n}, \quad a = .001, \quad n = 40 \tag{37}$$

If only rough guesses for C_e and T_e are available at the start of the computation, the iteration process of both coupled boundary-value problems suffers from an instability which could be cured by relaxing the newest value of T_e:

$$T_{e_{s+1}} = \alpha T_{e_s} + (1-\alpha)\, \tilde{T}_{e_{s+1}}, \tag{38}$$

in which s is the number of iterations and $\tilde{T}_e$ is the result of the quasi-Newton-Raphson process.

For the other quantities, the results could be accepted for each iteration step without relaxation. It appeared that, at the starting station only the relaxation parameter α had to satisfy: $.95 \leqslant \alpha < 1$.

The set of equations (32) through (36) is solved with the tuned program for the cathode wall under the following conditions: current crossing the channel $J_y = -10^4 A/m^2$, the emission current $J_{em} = -1.03\ 10^4 A/m^2$, magnetic field strength B=1 Tesla. It is assumed that the gasdynamic quantities satisfy the equation of state and at the centerline satisfy also the simplified continuity and momentum equation: $p = \rho RT$,

$$\frac{d}{dx}(\rho_c u_c) = 0, \tag{39}$$

$$\rho_c u_c \frac{du_c}{dx} + \frac{dp}{dx} = J_y . B.$$

T, ρ/ρ_c, u/u_c are given functions of y only (fig. 4), while no pressure variation in y-direction is present. At the duct entrance, x=0, the following values are given: velocity at the centerline u_{co}= 400 m/s, temperature at the centerline T_{co} = 1890 K, temperature at the wall T_{wo}=1600 K and pressure p_o = 1.5 bar.

Fig. 5 shows the chosen variation of u_c and ρ_c along the duct. At the initial position x=0.1 the starting profiles for T_e and C_e were found from a simplified form of the continuity and energy equation (32) and (33), in which convective terms are neglected.

In figures 6 and 7, results are depicted of C_e- and T_e-profiles. In figure 8 a detailed picture is shown of the effective electrical conductivity σ_{eff}. The electron concentration shows sharp peaks close to the wall. This effect is caused by the emission of electrons by the cathode (J_{em}). It should be emphasised that the model does not permit the existence of space charge, i.e. the number density of ions equals the number density of electrons. The electron temperature T_e increases with x, due to the decrease of ρ (fig. 5) that causes less energy transfer from the electrons to the heavy particles by means of collisions. This effect also gives rise to an increase in electron density. The behaviour of T_e near the wall is less obvious. The model of the boundary conditions at the wall yields for the energy of electrons passing the boundary between sheath and continuum plasma: $(Ee)_w = 2kT_e + e\Delta\varphi$, whereas the mean thermal energy of electrons in the continuum is given by $(Ee)_{cont} = {}^3/_2\ kT_e$. The influx of electrons from the cathode into the plasma is coupled with a net influx of energy to the electron gas, which is thermalized by electron-heavy particles collisions, thus increasing the local electron temperature. More refined models for the plasma-electrode interface are developed (ref. 16, 17) but should be accompanied by the introduction of as refined and more complicated models for the seperate components of the plasma. The computation from x=0.1 until x=2.0, required 190 sec. computer time at a CDC CYBER 72.

5. CONCLUSIONS

Two simple methods have been presented for the solution of parabolic differential equations. Both methods are fourth-order accurate in the space-like dimension and second-order accurate in the time-like dimension. In what is called the D-method, we increased the accuracy of a cubic-spline method by estimating the second-order truncation error by differentiating the basic equation twice. In the RH-method, a local Richardson-extrapolation is employed, before proceeding to the next x-station, to obtain fourth-order accurate values at every two points; subsequent quintic Hermite interpolation is then used to increase the accuracy of the remaining points. The boundary-layer flow near a stagnation point has been computed with both methods, and, for comparison, also with a cubic-spline method and with a pure difference method. From a von Neumann stability analysis applied to the internal points, it is inferred that the RH-method is unconditionally stable. The D-method has the same stability characteristics as the second-order cubic-spline method, which is also unconditionally stable.

The electron gas equations in an MHD-channel are considered to be of sufficient complexity to show the usefullness of the RH-method for practical parabolic problems. The equations are highly non-linear, and the boundary conditions at the cathode wall are functions of the electron gas concentration and temperature as well as of their derivatives. The corresponding computer program required some tuning, which included a transformation to stretch the y-coordinate near the wall, and the introduction of a relaxation process to cope with the high non-linearity of the energy equation. The results suggest that possibly a more refined model for the plasma-electrode interface is to be considered in the future. The RH-method can be regarded as a suitable tool to solve boundary-layer duct flows as well as other complicated parabolic problems.

6. REFERENCES

1. Snel,H., Lindhout,J.P.F., Merck,W.F.H., Houben,J., "Two dimensional MHD duct flow: numerical analysis and measurements", Proceedings of the sixth International Conference on Magnetic-Hydrodynamic Electrical Power Generation, Washington D.C., june 1974.
2. Rubin, S.G. and Graves Jr., R.A., "Viscous flow solutions with a cubic-spline approximation", Computers and Fluids, vol. 3, 1975, pp 1-36.
3. Daniel, J.W. and Swartz, B.K., "Extrapolated collocation for two point boundary value problems using cubic splines", Journal of the Institute of Mathematics and it Applications, vol. 16, 1975, pp 161-174.
4. Rubin, S.G. and Khosla, P.K., "Higher-order numerical solutions using cubic splines", AIAA Journal, vol. 14, no. 7, 1976, pp 851-858.
5. Schlichting, H., "Boundary Layer Theory", Mc. Graw-Hill, 1960.
6. Ahlberg, J.H., Nilson, E.N., Walsh, J.L., "The theory of splines and their applications", Academic Press, 1967.
7. Keller, H.B., "Some computational problems in boundary layer flows", Proceedings of the fourth international conference on Numerical Methods in Fluid Dynamics, Springer Verlag, june 1974.
8. Richtmeyer, R.D., Morton, K.W., "Difference methods for initial-value problems", John Wiley & Sons, 1967.

9. Sutton, G.W. and Sherman, A., "Engineering Magnetohydrodynamics", Mc. Graw-Hill, 1965.

10. Kerrebrock, J.L., Second Symposium on Engin. Asp. of MHD, p. 327, Columbia University Press, New York, 1962.

11. Brederlow, G. and Witte, K.J., "Effective Electrical Conductivity and Related Properties of a Non-eq. High Pressure MHD Plasma", AIAA-Journal, 12, 1, 1974.

12. Veefkind, A., "Non-equilibrium Phenomena in a Disc-shaped Magneto-hydrodynamic Generator", Thesis E.U.T., Eindhoven, 1970.

13. Merck, W.F.H. and Vroomen, L.H.J., Internal Report EGW/75/136, E.U.T., Eindhoven, 1975.

14. Merck, W.F.H. and Toussaint, P., Internal Report EGW/76/161, E.U.T., Eindhoven, 1976.

15. Sherman, A. and Reskotko, E., "Non-equilibrium Boundary Layer along an Insulator Wall", AIAA-Journal, 7, 4, 610, 1969.

16. Cott, D.W., "Ionizational and Electron Thermal Non-equilibrium Effects in Compressible MHD Boundary Layers", Thesis, University of Tennessee, Knoxville, 1969.

17. Koester, J.K., "Analytical and Experimental studies of Thermionically Emitting Electrodes in Contact with Dense, Seeded Plasmas", Cal. Inst. of Techn., Thesis, 1970.

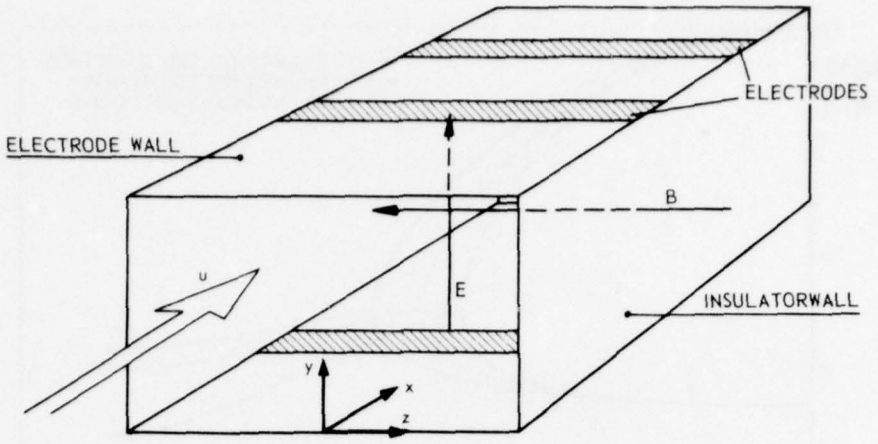

fig. 1 Schematic view of an MHD generator channel

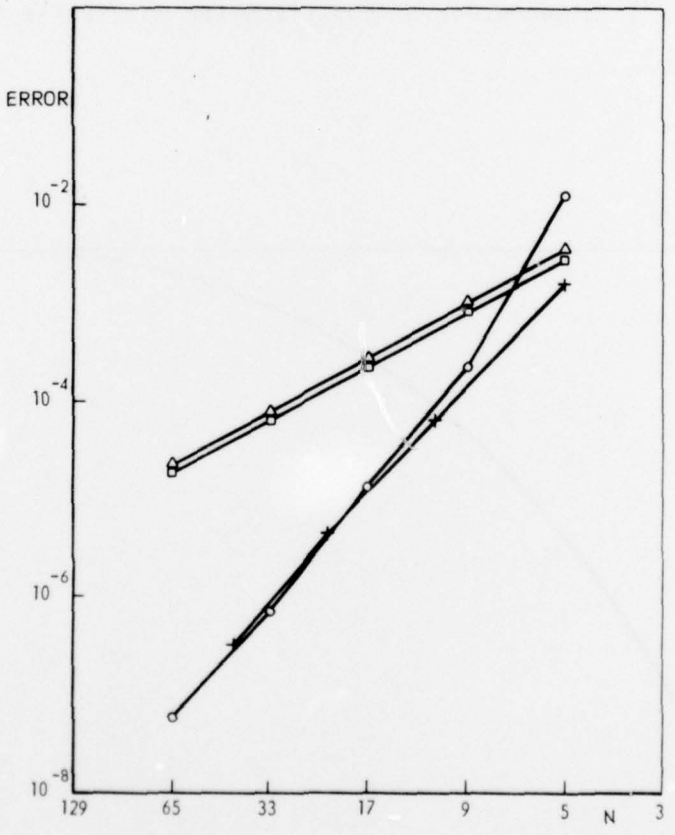

fig. 2 Accuracy for boundary layer flow; Δ, difference method; □, cubic-splines; O, reduction of truncation error by locally applied Richardson-extrapolation; +, reduction of truncation error by differentiation; N=number of points along normal

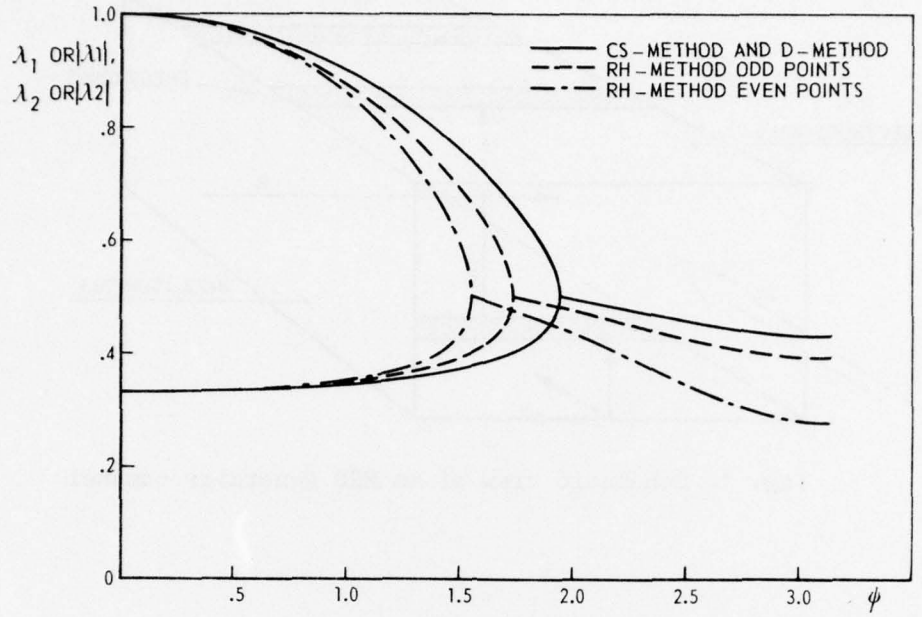

fig. 3 Eigenvalues of amplification matrix for $(k/h^2)\,\sigma = .1$

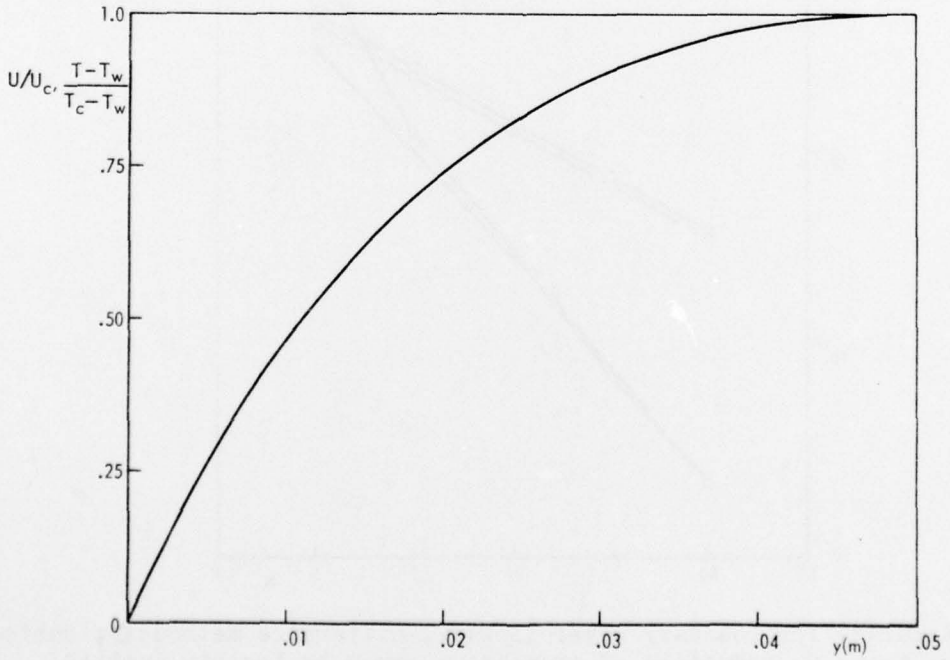

fig. 4 Given velocity and temperature profile.
x=0: u_c=400 m/s; T_c=1890 K; T_w=1600 K

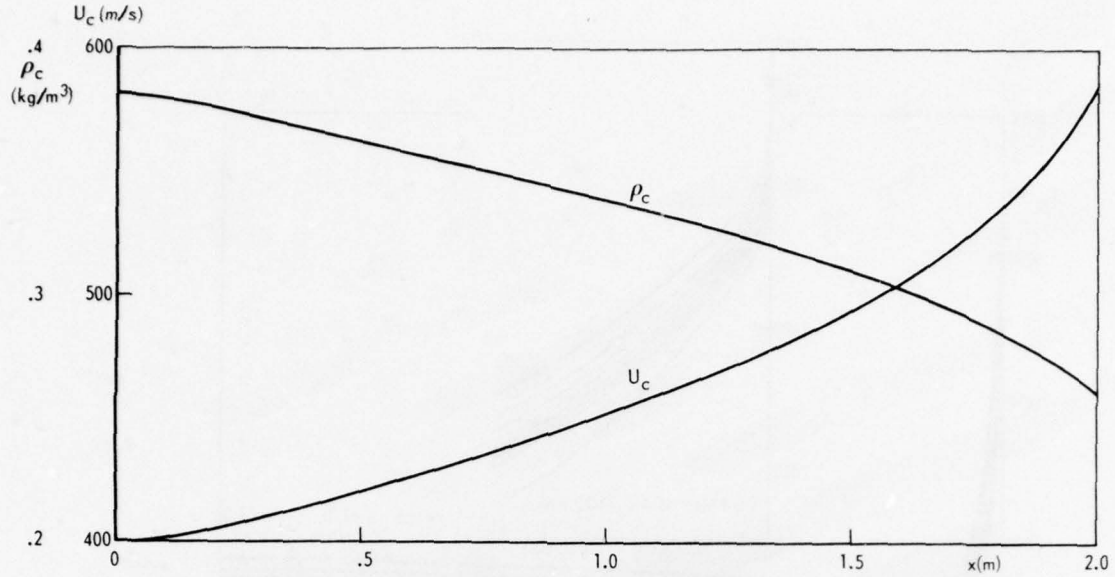

fig. 5 Variation of velocity and density along the centerline of the duct under influence of the Lorentz-force

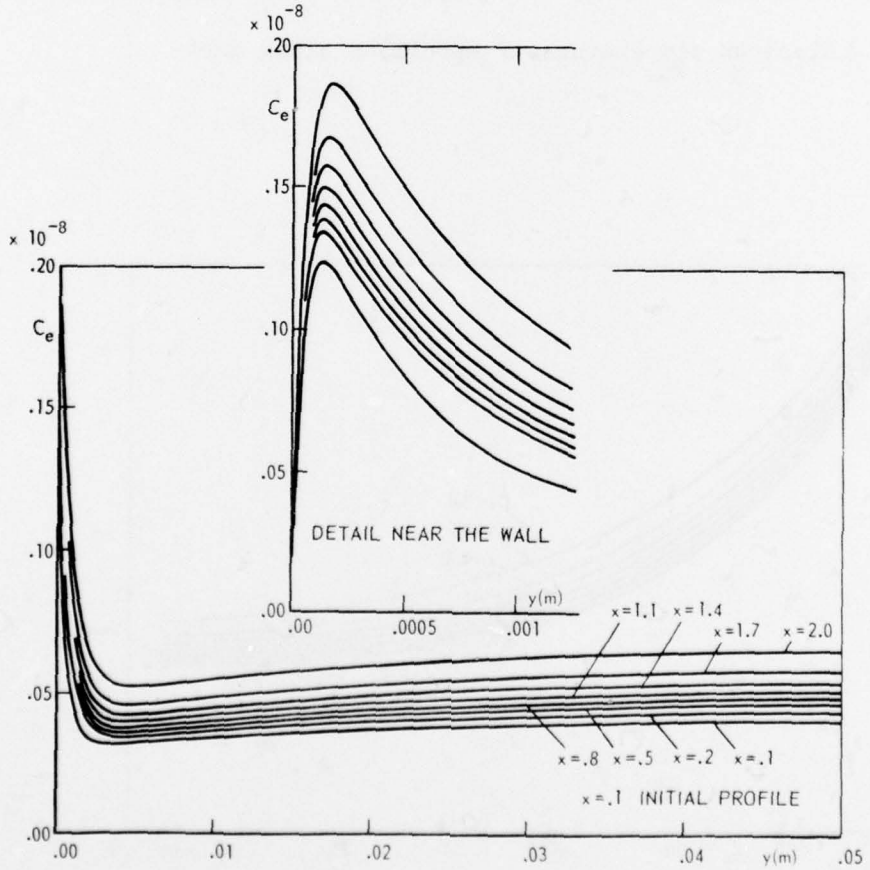

fig. 6 Electron concentration, C_e-profiles along duct

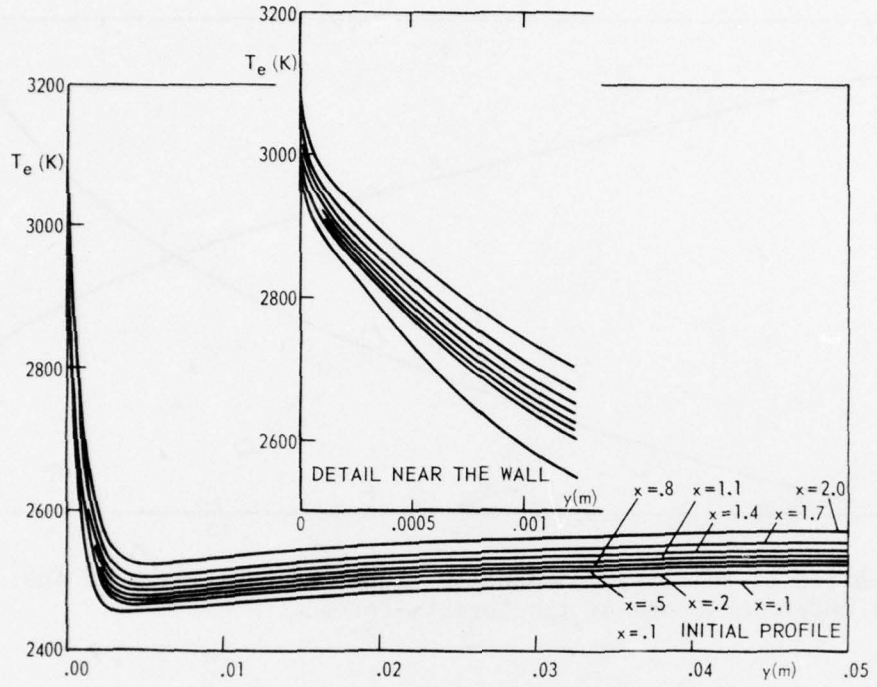

fig. 7 Electron temperature, T_e-profiles along duct

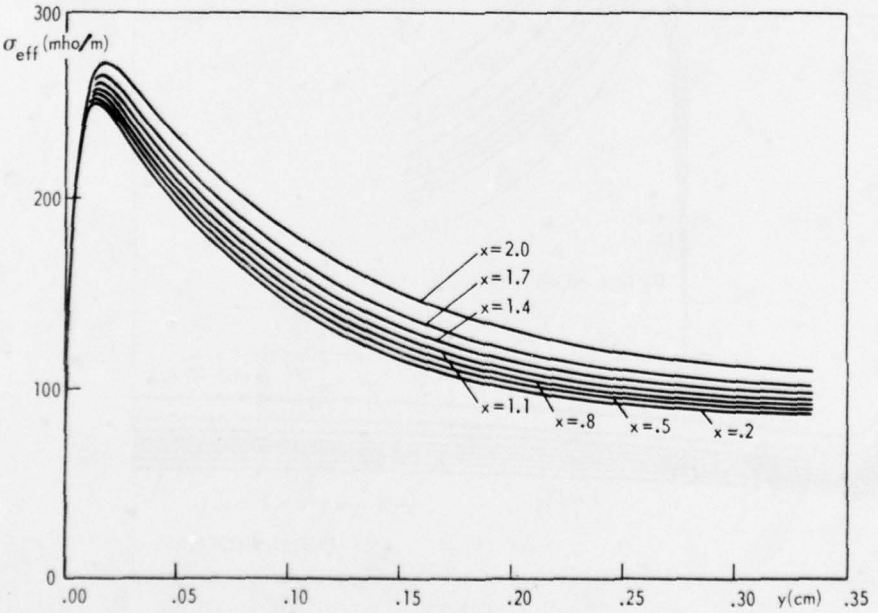

fig. 8 Detail of conductivity variation near the wall

$_{i+1}$,

$^{j+1}_{i-1}$). (21)

stigated by the von Neumann
heme, the analysis leads to a
3). The Fourier-decomposition of

(22)

he wave number. Substitution of
n $\xi_{1_{i+1}}$, ξ_{1_i} and $\xi_{1_{i-1}}$ which
n by the introduction of ξ_2:

(23)

r:

(24)

$\Big)$ and $\xi = (\xi_1, \xi_2)^T$,

h.